Inorganic Chemistry
Article

Inorg. Chem. **2009**, *48*, 6713–6723 **6713**
DOI: 10.1021/ic900645d

Tridecanuclear $[Mn^{III}_5Ln^{III}_8]$ Complexes Derived from *N*-^{t}Butyl-diethanolamine: Synthesis, Structures, and Magnetic Properties

Ayuk M. Ako,[†,‡] Valeriu Mereacre,[†] Rodolphe Clérac,[*,§,∥] Ian J. Hewitt,[†] Yanhua Lan,[†] Gernot Buth,[⊥] Christopher E. Anson,[†] and Annie K. Powell[*,†,‡]

[†]*Institut für Anorganische Chemie der Universität Karlsruhe, Engesserstrasse 15, Karlsruhe Institute of Technology, D-76131 Karlsruhe, Germany,* [‡]*Institute for Nanotechnology, Forschungszentrum Karlsruhe, Karlsruhe Institute of Technology, Postfach 3640, D-76021 Karlsruhe, Germany,* [§]*CNRS, UPR 8641, Centre de Recherche Paul Pascal (CRPP), Equipe "Matériaux Moléculaires Magnétiques", 115 avenue du Dr. Albert Schweitzer, Pessac F-33600, France,* [∥]*Université de Bordeaux, UPR 8641, Pessac F-33600, France, and* [⊥]*Institut für Synchrotronstrahlung, Forschungszentrum Karlsruhe, D-76344 Eggenstein-Leopoldshafen, Germany*

Received April 2, 2009

The synthesis, structures and magnetic properties of a family of heterometallic $[Mn^{III}_5Ln^{III}_8(\mu_3\text{-}OH)_{12}(L^2)_4(piv)_{12}(NO_3)_4(OAc)_4]^-$ (Ln = Pr, **2**; Nd, **3**; Sm, **4**; Gd, **5**; Tb, **6**) aggregates are reported. The complexes were obtained from the direct reaction of *N*-^{t}butyldiethanolamine (H_2L^2) with $Mn(OAc)_2\cdot 4H_2O$ and $Ln(NO_3)_3\cdot 6H_2O$ in the presence of pivalic acid (pivH) in MeCN under ambient conditions. Compounds **2**−**6** are isomorphous and crystallize in the monoclinic space group $P2_1/n$ with four molecules in the unit cell. The complexes have a centrosymmetric tridecanuclear anionic core consisting of two distorted inner heterometallic $[Mn^{III}Ln^{III}_3(\mu_3\text{-}OH)_4]^{8+}$ cubane subunits sharing a common Mn vertex flanked by four edge-sharing heterometallic $[Mn^{III}Ln^{III}_2(\mu_3\text{-}OH)_4]^{5+}$ defect cubane units. Complexes **2**−**6** are the first high-nuclearity 3d-4f aggregates reported to date using ^{t}Bu-deaH$_2$ as ligand. These compounds show no evidence of slow relaxation behavior above 1.8 K, which appears to be the consequence of the very weak or non-existent magnetic interactions between the Mn^{III} and Ln^{III} ions resulting from the particular angles at the bridging oxygens.

Introduction

In the past few decades, the synthesis and characterization of 3d metal complexes have been the focus of intense research activity for a variety of reasons. These include the structural beauty of some of these species and the synthetic challenge involved in obtaining them. More importantly, some of these complexes exhibit interesting magnetic properties such as single-molecule magnet (SMM) behavior.[1] SMMs are individual molecules that behave as magnets below a certain blocking temperature[2] with potential applications in the information storage industry or as qubits in quantum computing.[3] In general, prerequisites for SMM behavior are a combination of high (or at least nonzero) ground spin state (S) and a large uniaxial anisotropy of an Ising type which can be a result of a favorable zero-field splitting parameter, D, or in the case of lanthanide ions an overall anisotropy parameter.[4] The energy barrier to the reversal of the molecular spin in the ground state (S_T) should be generated in the form of $\Delta = |D|S_T^2$ for integer spin and $|D|(S_T^2 - {}^1/_4)$ for half-integer spin, although a recent reappraisal of this suggests that the relationship is linearly dependent on the spin S_T.[5] For these reasons, complexes containing the high spin Mn^{III} ion, with its large ground state spin and uniaxial anisotropy, have received increasing attention since the initial discovery of the SMM phenomenon, and complexes with nuclearity as

*To whom correspondence should be addressed. E-mail: clerac@crpp-bordeaux.cnrs.fr (R.C.), powell@aoc.uni-karlsruhe.de (A.K.P.). Fax: +49 721 608 8142 (A.K.P.). Phone: +49 721 608 2135 (A.K.P.).

(1) (a) Christou, G.; Gatteschi, D.; Hendrickson, D. N.; Sessoli, R. *MRS Bull.* **2000**, *25*, 66. (b) Aromi, G.; Brechin, E. K. *Struct. Bonding (Berlin)* **2006**, *122*, 1. (c) Gatteschi, D.; Sessoli, R. *Angew. Chem., Int. Ed.* **2003**, *42*, 268. (d) Chakov, N. E.; Lee, S.-C.; Harter, A. G.; Kuhns, P. L.; Reyes, A. P.; Hill, S. O.; Dalal, N. S.; Wernsdorfer, W.; Abboud, K. A.; Christou, G. *J. Am. Chem. Soc.* **2006**, *128*, 6975. (e) Bagai, R.; Abboud, K. A.; Christou, G. *Inorg. Chem.* **2007**, *46*, 5567.

(2) (a) Bircher, R.; Chaboussant, G.; Dobe, C.; Güdel, H. U.; Ochsenbein, S. T.; Sieber, A.; Waldmann, O. *Adv. Funct. Mater.* **2006**, *16*, 209. (b) Gatteschi, D.; Sessoli, R. *Angew. Chem., Int. Ed.* **2003**, *42*, 268. (c) Aubin, S. M. J.; Gilley, N. R.; Pardi, L.; Krzystek, J.; Wemple, M. W.; Brunel, L.-C.; Maple, M. B.; Christou, G.; Hendrickson, D. N. *J. Am. Chem. Soc.* **1998**, *120*, 4991. (d) Oshio, H.; Nakano, M. *Chem.—Eur. J.* **2005**, *11*, 5178.

(3) (a) Bogani, L.; Wernsdorfer, W. *Nat. Mater.* **2008**, *7*, 179. (b) Leuenberger, M. N.; Loss, D. *Nature* **2001**, *414*, 789.

(4) (a) Soler, M.; Wernsdorfer, W.; Folting, K.; Pink, M.; Christou, G. *J. Am. Chem. Soc.* **2004**, *126*, 2156. (b) Murugesu, M.; Habrych, M.; Wernsdorfer, W.; Abboud, K. A.; Christou, G. *J. Am. Chem. Soc.* **2004**, *126*, 4766. (c) Wittick, L. M.; Murray, K. S.; Moubaraki, B.; Batten, S. R.; Spiccia, L.; Berry, K. J. *Dalton Trans.* **2004**, 1003. (d) Tasiopoulos, A. J.; Wernsdorfer, W.; Moulton, B.; Zaworotko, M. J.; Christou, G. *J. Am. Chem. Soc.* **2004**, *125*, 15274.

(5) Waldmann, O. *Inorg. Chem.* **2007**, *46*, 10035.

Published on Web 06/16/2009

high as [Mn_{84}] have been reported.[6] Although the Mn^{III} ion is the most widely known source of the required anisotropy, SMMs incorporating $Fe^{II/III}$, Co^{II}, Ni^{II}, and lanthanide ions have also been reported.[7,8] Thus, it would seem that mixed-metal systems containing both Mn^{III} ions (having a d^4 configuration, $S = 2$ ground state spin and a zero-field splitting) and lanthanide ions (which generally show significant single-ion anisotropy) should be promising candidates for the development of molecular species that exhibit slow relaxation of the magnetization, that is, SMMs. While such a combination of 3d and 4f spin carriers within a given complex does not always yield SMMs,[9] the systematic study of such molecular systems provides valuable insights into the magnetic interactions, the correlation of these with structural parameters, and the conditions necessary for producing SMM behavior.

The generation of isostructural inorganic−organic frameworks is another important aspect of this type of research work as it allows for a systematic and comparative study of properties. In particular, the magnetic properties of such architectures can be tuned by changing the nature of the metal centers and to some extent the ligands or ligand periphery.[10,11] For instance, recently Christou and co-workers were able to maximize the spin ground state of a known metal-centered hexagonal topology through targeted structural perturbation.[12] Moreover, by combining different metal ions, it should be possible to prepare molecules with larger magnetic anisotropy and/or higher spin ground states as a result of ferro- or antiferro-magnetic interactions between the spin carriers.

To date, there have been few reports of heterometallic [Mn−Ln] systems with nuclearity exceeding 10 metal centers. The few documented cases include [$Mn_4^{III}Mn_2^{IV}Dy_6^{III}$], reported by Pecoraro and co-workers,[13] [$Mn_{11}^{III}Dy_4^{III}$], [$Mn_{10}^{III}Ce_2^{III}Ce_2^{IV}$], [$Mn_{11}^{III}Mn^{II}Gd^{III}$], reported by Christou et al.,[14] and [$Mn_9^{III}Mn_2^{II}Gd_2^{III}$], [$Mn_{12}^{III}Mn_6^{II}Dy^{III}$] reported by our group,[15] which, with the exception of the [$Mn_{10}^{III}Ce_2^{III}Ce_2^{IV}$] complex, are all SMMs. Therefore, further examples of high-nuclearity [Mn−Ln] complexes should help to improve our understanding of the magnetic exchange interactions between transition metals and lanthanide ions in larger aggregates.

Alkoxy ligands are widely employed in the synthesis of high nuclearity complexes because they possess chelating and bridging capabilities.[16] While significant progress has been made in the use of diethanolamine ligands and other related tripodal ligands in the synthesis of high spin Mn complexes,[17] there are only limited examples of mixed-metal complexes derived from this class of ligands in the literature.[18,19] Along these lines, Hendrickson, Tong, and co-workers recently reported a giant heterometallic [$Cu_{17}Mn_{28}$] aggregate with T_d symmetry and high spin ground state, obtained using triethanolamine.[20] The reactivity of diethanolamine ligands depends on their degree of deprotonation (Scheme 1) which in turn depends on the reaction conditions. When proto-

(6) (a) Sessoli, R.; Tsai, H.-L.; Schake, A. R.; Wang, S.; Vincent, J. B.; Folting, K.; Gatteschi, D.; Christou, G.; Hendrickson, D. N. *J. Am. Chem. Soc.* **1993**, *115*, 1804. (b) Tasiopoulos, A. J.; Vinslava, A.; Wernsdorfer, W.; Abboud, K. A.; Christou, G. *Angew. Chem., Int. Ed.* **2004**, *43*, 2117.

(7) (a) Ferbinteanu, M.; Miyasaka, H.; Wernsdorfer, W.; Nakata, K.; Sugiura, K. M.; Yamashita, M.; Coulon, C.; Clérac, R. *J. Am. Chem. Soc.* **2005**, *127*, 3090. (b) Toma, L. M.; Lescouëzec, R.; Pasán, J.; Ruiz-Pérez, C.; Vaissermann, J.; Cano, J.; Carrasco, R.; Wernsdorfer, W.; Lloret, F.; Julve, M. *J. Am. Chem. Soc.* **2006**, *128*, 4842. (c) Bernot, K.; Bogani, L.; Caneschi, A.; Gatteschi, D.; Sessoli, R. *J. Am. Chem. Soc.* **2006**, *128*, 7947. (d) Caneschi, A.; Gatteschi, D.; Lalioti, N.; Sangregorio, C.; Sessoli, R.; Venturi, G.; Vindigni, A.; Rettori, A.; Pini, M. G.; Novak, M. A. *Angew. Chem., Int. Ed.* **2001**, *40*, 1760.

(8) (a) Bogani, L.; Sangregorio, C.; Sessoli, R.; Gatteschi, D. *Angew. Chem., Int. Ed.* **2005**, *44*, 5817. (b) Li, X.-J.; Wang, X.-Y.; Gao, S.; Cao, R. *Inorg. Chem.* **2006**, *45*, 1508. (c) Lecren, L.; Roubeau, O.; Coulon, C.; Li, Y.-G.; Le Goff, X. F.; Wernsdorfer, W.; Miyasaka, H.; Clérac, R. *J. Am. Chem. Soc.* **2005**, *127*, 17353. (d) Zheng, Y.-Z.; Tong, M.-L.; Zhang, W.-X.; Chen, X.-M. *Angew. Chem., Int. Ed.* **2006**, *45*, 6310. (e) Bai, Y.-L; Tao, J.; Wernsdorfer, W.; Sato, O.; Huang, R.-B.; Zheng, L.-S. *J. Am. Chem. Soc.* **2006**, *128*, 16428. (f) Madalan, A. M.; Avarvari, N.; Fourmigué, M.; Clérac, R.; Chibotaru, L. F.; Clima, S.; Andruh, M. *Inorg. Chem.* **2008**, *47*, 940. (g) Pointillart, F.; Bernot, K.; Sessoli, R.; Gatteschi, D. *Chem.—Eur. J.* **2007**, *13*, 1602.

(9) (a) Wu, G.; Hewitt, I. J.; Mameri, S.; Lan, Y.; Clérac, R.; Anson, C. E.; Qiu, S.; Powell, A. K. *Inorg. Chem.* **2007**, *46*, 7229. (b) Lampropoulos, Ch.; Stamatatos, Th. C.; Abboud, K. A.; Christou, G. *Inorg. Chem.* **2009**, *48*, 429. (c) Alley, K. G.; Mukherjee, A.; Clérac, R.; Boskovic, C. *Dalton Trans* **2008**, 59.

(10) (a) Milios, C. J.; Inglis, R.; Bagai, R.; Wernsdorfer, W.; Collins, A.; Moggach, S.; Parsons, S.; Perlepes, S. P.; Christou, G.; Brechin, E. K. *Chem. Commun.* **2007**, 3476, and references therein. (b) Li, D.; Parkin, S.; Wang, G.; Yee, G. T.; Clérac, R.; Wernsdorfer, W.; Holmes, S. M. *J. Am. Chem. Soc.* **2001**, *128*, 4214. (c) Miyasaka, H.; Clérac, R.; Mizushima, K.; Sugiura, K.; Yamashita, M.; Wernsdorfer, W.; Coulon, C. *Inorg. Chem.* **2003**, *42*, 8203. (d) Boskovic, C.; Pink, M.; Huffman, J. C.; Hendrickson, D. N.; Christou, G. *J. Am. Chem. Soc.* **2001**, *123*, 9914. (e) Yang, C.-I.; Tsai, H.-L.; Lee, G.-H.; Wur, C.-S.; Yang, S.-F. *Chem. Lett.* **2005**, *34*, 288. (f) Schake, A. R.; Tsai, H.-L.; Webb, R. J.; Folting, K.; Christou, G.; Hendrickson, D. N. *Inorg. Chem.* **1994**, *33*, 6020.

(11) (a) Stamatatos, Th. C.; Abboud, K. A.; Wernsdorfer, W.; Christou, G. *Angew. Chem., Int. Ed.* **2007**, *46*, 884. (b) Boudalis, A. K.; Sanakis, Y.; Clemente-Juan, J. M.; Donnadieu, B.; Nastopoulos, V.; Mari, A.; Coppel, Y.; Tuchagues, J.-P.; Perlepes, S. P. *Chem.—Eur. J.* **2008**, *14*, 2514. (c) Inglis, R.; Jones, L. F.; Mason, K.; Collins, A.; Moggach, S. A.; Parsons, S.; Perlepes, S. P.; Wernsdorfer, W.; Brechin, E. K. *Chem.—Eur. J.* **2008**, *14*, 9117.

(12) Stamatatos, Th. C.; Poole, K. M.; Foguet-Albiol, D.; Abboud, K. A.; O'Brien, T. A.; Christou, G. *Inorg. Chem.* **2008**, *47*, 6593.

(13) Zaleski, C. M.; Depperman, E. C.; Kampf, J. W.; Kirk, M. L.; Pecoraro, V. L. *Angew. Chem., Int. Ed.* **2004**, *43*, 3912.

(14) (a) Mishra, A.; Wernsdorfer, W.; Abboud, K. A.; Christou, G. *J. Am. Chem. Soc.* **2004**, *126*, 15648. (b) Mishra, A.; Tasiopoulos, A. J.; Wernsdorfer, W.; Abboud, K. A.; Christou, G. *Inorg. Chem.* **2007**, *46*, 3105. (c) Stamatatos, Th. C.; Teat, S. J.; Wernsdorfer, W.; Christou, G. *Angew. Chem., Int. Ed.* **2009**, *48*, 521.

(15) (a) Mereacre, V. M.; Ako, A. M.; Clérac, R.; Wernsdorfer, W.; Filoti, G.; Bartolomé, J.; Anson, C. E.; Powell, A. K. *J. Am. Chem. Soc.* **2007**, *129*, 9248. (b) Ako, A. M.; Mereacre, V. M.; Clérac, R.; Wernsdorfer, W.; Hewitt, I. J.; Anson, C. E.; Powell, A. K. *Chem Commun.* **2009**, 544.

(16) (a) Rumberger, E. M.; Shah, S. J.; Beedle, C. C.; Zakharov, L. N.; Rheingold, A. L.; Hendrickson, D. N. *Inorg. Chem.* **2005**, *44*, 2742, and references therein. (b) Murugesu, M.; Habrych, M.; Wernsdorfer, W.; Abboud, K. A.; Christou, G. *J. Am. Chem. Soc.* **2004**, *126*, 4766. (c) Boskovic, C.; Wernsdorfer, W.; Folting, K.; Huffmann, J. C.; Hendrickson, D. N.; Christou, G. *Inorg. Chem.* **2002**, *41*, 5107. (d) Glaser, T.; Liratzis, I.; Lügger, T.; Fröhlich, R. *Eur. J. Inorg. Chem.* **2004**, 2683, and references therein. (e) Yang, C. I.; Lee, G. H.; Wur, C. S.; Lin, J. G.; Tsai, H. L. *Polyhedron* **2005**, *24*, 2215.

(17) (a) Saalfrank, R. W.; Scheurer, A.; Prakash, R.; Heinemann, F. W.; Nakajima, T.; Hampel, F.; Leppin, R.; Pilawa, B.; Rupp, H.; Müller, P. *Inorg. Chem.* **2007**, *46*, 1586, and references therein. (b) Manoli, M.; Prescimone, A.; Bagai, R.; Mishra, A.; Murugesu, M.; Parsons, S.; Wernsdorfer, W.; Christou, G.; Brechin, E. K. *Inorg. Chem.*, **2007**, *46*, 6968, and references therein. (c) Rajaraman, G.; Murugesu, M.; Sanudo, E. C.; Soler, M.; Wernsdorfer, W.; Helliwell, M.; Muryn, C.; Raftery, J.; Teat, S. J.; Christou, G.; Brechin, E. K. *J. Am. Chem. Soc.* **2004**, *126*, 15445.

(18) Wang, W. -G.; Zhou, A.; Zhang, W. -X.; Tong, M. -L.; Chen, X. -M.; Nakano, M.; Beedle, C. C.; Hendrickson, D. N. *J. Am. Chem. Soc.* **2007**, *129*, 1014, and references therein.

(19) (a) Mereacre, V. M.; Ako, A. M.; Clérac, R.; Wernsdorfer, W.; Hewitt, I. J.; Anson, C. E.; Powell, A. K. *Chem.−Eur. J.* **2008**, *14*, 3577. (b) Saalfrank, R. W.; Prakash, R.; Maid, H.; Hampel, F.; Heinemann, F. W.; Trautwein, A. X.; Böttger, L. H. *Chem.−Eur. J.* **2006**, *12*, 2428.

(20) Wang, W.-G.; Zhou, A.-J.; Zhang, W. -X.; Tong, M. -L.; Chen, X.-M.; Nakano, M.; Beedle, C. C.; Hendrickson, D. N. *J. Am. Chem. Soc.* **2007**, *129*, 1014.

Scheme 1. (Top) Reactive Forms of Diethanolamine Ligands;[a] (Bottom Left) *N*-^{n}Butyldiethanolamine (H_2L^1); (Bottom Right) *N*-^{t}Butyldiethanolamine (H_2L^2)

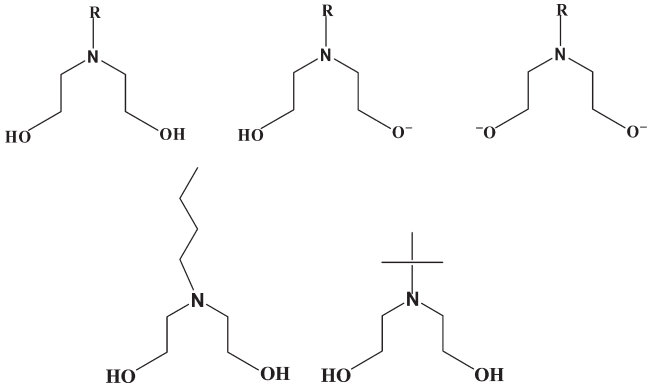

[a] R = Substituent. Left: protonated form. Center: singly deprotonated form. Right: doubly deprotonated form.

Scheme 2. Coordination of *N*-Substituted Diethanolamines in Partially or Doubly Deprotonated Mode to 3d−4f Metal Ions[a]

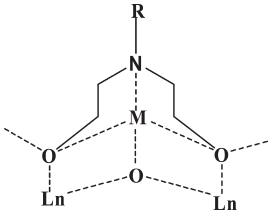

[a] R = Substituent; M = 3d metal ion; Ln = 4f metal ion.

nated, mononuclear species are usually formed, while when partially or doubly deprotonated, coordination to metal ions yields oligomeric products.

The chemical characteristics of the tridentate (N,O,O) diethanolamine ligands makes them particularly suitable for 3d-4f coordination chemistry. They can indeed be considered as coded for coordination of both 3d and 4f metal ions. In coordination to 3d-4f metal ions the soft donor N atom of the N,O,O chelate is likely to bind to the comparatively softer transition metal ions while the hard donor O atoms of the diethanolamine ligands will ligate the harder, oxophilic lanthanide ions, as well as providing bridging to other metal centers (Scheme 2). Further bridging can be provided by ancillary ligands, such as carboxylate, which also serve to occupy the remaining coordination sites on the metal ions.

As part of our exploration of synthetic strategies for creating mixed d/f spin aggregates,[9a,10,19a,21,22] we have employed preformed complexes, as well as *N*-substituted diethanolamines or related tripodal ligands in the synthesis of high-nuclearity 3d-4f compounds. We reported the synthesis, structures, and magnetic properties of $[Mn_xLn_y]$,[15,19a,21] $[Cu^{II}_5Gd^{III}_2]$,[9] and the tridecanuclear $[Fe^{III}_5Ln^{III}_8]$ (Ln = Pr

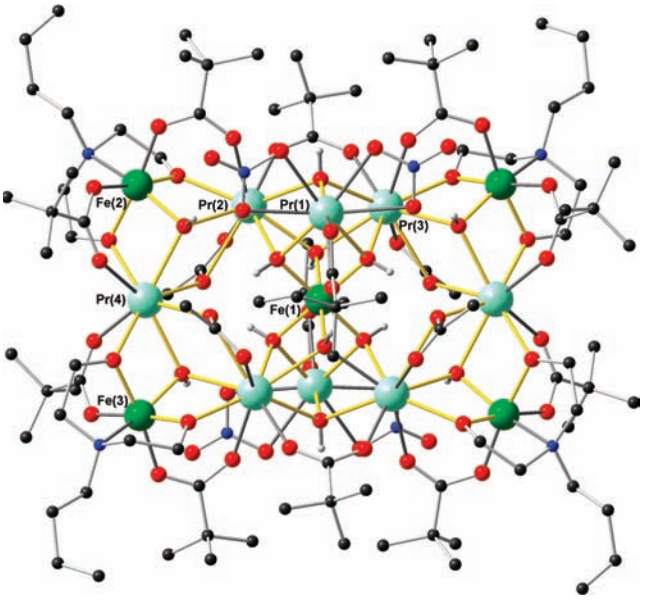

Figure 1. Molecular structure of the anion $[Fe^{III}_5Pr_8(\mu_3\text{-}OH)_{12}(L^1)_4(piv)_{12}(NO_3)_4(OAc)_4]^-$ in **1a**.[22] Color code: Fe (green), Pr (light green), N (blue), O (red), C (black).

(**1a**), Nd (**1b**), Gd(**1c**)) complexes.[22] The $[Fe^{III}_5Ln^{III}_8]$ system (Figure 1) was obtained from the reaction of the well-known iron(III) pivalate triangle $[Fe_3O(O_2CCMe_3)_6(H_2O)_3]O_2CCMe_3$ with *N*-^{n}Butyldiethanolamine (^{n}Bu-deaH$_2$ or H_2L^1), $Ln(NO_3)_3\cdot 6H_2O$ and $NaOAc\cdot 3H_2O$ in MeCN. The $[Fe^{III}_5Ln^{III}_8]$ aggregates showed high spin ground states but no slow relaxation of the magnetization was observed above 1.8 K. It was therefore of interest to synthesize isostructural Mn^{III} analogues of these aggregates, as replacement of isotropic $3d^5$ Fe^{III} by $3d^4$ Mn^{III} with its Jahn−Teller distortion might be a way of introducing additional magnetic anisotropy to the system. This synthesis seemed promising, considering that Fe^{III} and Mn^{III} have similar ionic radii and hence coordination chemistry. While α-methylene diethanolamines have been extensively employed in the synthesis of homometallic and heterometallic clusters,[19b,23,24] the α-branched, sterically bulkier *N*-^{t}Butyldiethanolamine (^{t}BudeaH$_2$ or H_2L^2, Scheme 1) has rarely been used in cluster chemistry, although Saalfrank and co-workers successfully employed H_2L^2 in the synthesis of mixed-valent octanuclear iron defect hexacubane complexes and a (CaCl)-capped nonanuclear body-centered six-sided iron(III) polyhedron.[25] Given that we have already established that using the related ligand *N*-methyldiethanolamine in a Mn/Ln system results in the formation of nonanuclear $[Mn_5Ln_4]$ compounds,[19a] we decided to carry out an extension of our previous work on the $[Fe^{III}_5Ln^{III}_8]$ system by employing the isomeric but sterically bulkier *N*-^{t}Butyldiethanolamine (H_2L^2) to synthesize the

(21) (a) Mereacre, V.; Prodius, D.; Ako, A. M.; Kaur, N.; Lipkowski, J.; Simmons, C.; Dalal, N.; Geru, I.; Anson, C. E.; Powell, A. K.; Turta, C. *Polyhedron* **2008**, *27*, 2459. (b) Akhtar, M. N.; Zheng, Y.-Z.; Lan, Y.; Mereacre, V.; Anson, C. E.; Powell, A. K. *Inorg. Chem.* **2009**, *48*, 3015. (c) Akhtar, M. N.; Lan, Y.; Mereacre, V.; Clérac, R.; Anson, C. E.; Powell, A. K. *Polyhedron* **2009**, *28*, 1698.

(22) Ako, A. M.; Mereacre, V.; Clérac, R.; Hewit, I. J.; Lan, Y.; Anson, C. E.; Powell, A. K. *Dalton Trans.* **2007**, 5245.

(23) (a) Wittick, L. M.; Murray, K. S.; Moubaraki, B.; Batten, S. R.; Spiccia, L.; Berry, K. J. *Dalton Trans.* **2004**, 1003. (b) Wittick, L. M.; Jones, L. F.; Jensen, P.; Moubaraki, B.; Spiccia, L.; Berry, K. L.; Murray, K. S. *Dalton Trans.* **2006**, 1534.

(24) (a) Murugesu, M.; Wernsdorfer, W.; Abboud, K. A.; Christou, G. *Angew. Chem., Int. Ed.* **2005**, *44*, 892. (b) Shah, S. J.; Ramsey, C. M.; Heroux, K. J.; DiPasquale, A. G.; Dalal, N. S.; Rheingold, A. L.; del Barco, E.; Hendrickson, D. N. *Inorg. Chem.* **2008**, *47*, 9569, and references therein.

(25) (a) Prakash, R.; Saalfrank, R. W.; Maid, H.; Scheurer, A.; Heinemann, F. W.; Trautwein, A. X.; Böttger, L. H. *Angew. Chem., Int. Ed.* **2006**, *45*, 5885. (b) Saalfrank, R. W.; Maid, H.; Scheurer, A. *Angew. Chem., Int. Ed.* **2008**, *47*, 8794.

Table 1. Crystallographic Data and Structure Refinement for Complexes **2**−**6**

compound	**2**	**3**	**4**	**5**	**6**
formula	$C_{118}H_{235}Mn_5N_{14}O_{66}Pr_8$	$C_{122}H_{241}Mn_5N_{16}Nd_8O_{66}$	$C_{124}H_{244}Mn_5N_{17}O_{66}Sm_8$	$C_{118}H_{235}Gd_8Mn_5N_{14}O_{66}$	$C_{120}H_{238}Mn_5N_{15}O_{66}Tb_8$
formula weight	4308.18	4416.93	4506.86	4438.90	4493.21
crystal system	monoclinic	monoclinic	monoclinic	monoclinic	monoclinic
space group	$P2_1/n$	$P2_1/n$	$P2_1/n$	$P2_1/n$	$P2_1/n$
a/Å	20.1817(5)	20.1037(8)	20.0283(9)	20.0032(6)	19.9081(7)
b/Å	28.5006(8)	28.3153(11)	28.3101(12)	28.2555(5)	27.9985(6)
c/Å	32.5851(7)	32.6441(14)	32.4451(14)	32.4417(8)	32.3927(11)
β/deg	103.001(2)	103.036(3)	102.851(1)	102.672(2)	102.764(3)
U/Å^3	18262.2(8)	18103.5(13)	17935.7(14)	17889.4(8)	17609.4(9)
Z	4	4	4	4	4
T/K	150	150	150	150	150
F(000)	8664	8872	9024	8824	8944
D_c/Mg m^{-3}	1.567	1.621	1.669	1.648	1.695
μ/mm^{-1}	3.394	3.668	4.107	3.341	4.958
λ/Å	0.80000	0.80000	0.80000	0.71073	0.80000
crystal size/mm	0.17 × 0.03 × 0.007	0.11 × 0.03 × 0.004	0.12 × 0.03 × 0.015	0.23 × 0.08 × 0.06	0.15 × 0.06 × 0.008
data measured	87009	113886	92829	128467	87450
unique data	28825	30387	30665	35196	28797
R_{int}	0.0919	0.1046	0.0311	0.0552	0.1159
Data with I ≥ 2σ(I)	22403	25034	28082	28023	22963
wR_2 (all data)	0.1253	0.1644	0.0829	0.1522	0.1943
S (all data)	1.053	1.085	1.030	1.014	1.088
R_1 [$I \geq 2\sigma(I)$]	0.0570	0.0624	0.0302	0.0570	0.0701
parameters/restraints	1785/61	1836/105	1878/67	1727/53	1743/63
biggest diff. peak/hole/eÅ^{-3}	+1.30/−1.13	+1.46/−1.46	+2.46/−0.88	+0.88/−2.72	+2.38/−2.66
CCDC no.	693908	693909	693910	693911	693912

[$Mn_5^{III}Ln_8^{III}$] analogues. We aimed by so doing among other reasons to assess the impact ligand bulk and metal center substitution (Mn^{III} ($3d^4$) for Fe^{III} ($3d^5$)) would have on the structural topology and the magnetic properties of the resulting aggregates. Moreover, the deliberate combination of the bulky H_2L^2 ligand with the bulky ancillary carboxylate ligand was aimed at minimizing intermolecular interactions of the resulting complexes in the crystal. As far we know, no heterometallic 3d-4f complex has so far been reported with this ligand.

Experimental Section

General Procedures. Unless otherwise stated all reagents were obtained from commercial sources, and were used as received, without further purification. All reactions were carried out under aerobic conditions. Elemental analyses for C, H and N were performed using an Elementar Vario EL analyzer and were carried out at the Institute of Inorganic Chemistry, University of Karlsruhe. FTIR spectra were measured on a Perkin-Elmer Spectrum One spectrometer with samples prepared as KBr discs.

Synthesis. $[Mn_5^{III}Ln_8^{III}(\mu_3\text{-}OH)_{12}(L^2)_4(piv)_{12}(NO_3)_4(OAc)_4]^-[H_3L^2]^+\cdot n$MeCN. General Method. A solution of *N*-^{t}Butyldiethanolamine (0.32 g, 2 mmol) in MeCN (5 mL) was gradually added to a stirred solution of $Mn(OAc)_2\cdot 4H_2O$ (0.025 g, 0.1 mmol), pivalic acid (0.071 g, 0.7 mmol), and $Ln(NO_3)_3\cdot 6H_2O$ (0.8 mmol) in MeCN (20 mL). The resulting brown solution was stirred under ambient conditions for 2 h and filtered. X-ray quality crystals of **2**−**6** were obtained after 48−72 h in yields of 36−63% as pale brown plates.

$[Mn_5Pr_8(\mu_3\text{-}OH)_{12}(L^2)_4(piv)_{12}(NO_3)_4(OAc)_4]^-[H_3L^2]^+\cdot$ 5MeCN (2·5MeCN). Yield: 33 mg (39% based on Mn). Anal. Calcd for $C_{108}H_{220}Mn_5N_9O_{66}Pr_8$ (dried): C, 31.61; H, 5.40; N, 3.07. Found: C, 31.96; H, 4.88; N, 3.21. Selected IR data (KBr disk): 3609 (s), 3383 (b), 2961 (s), 2866 (m), 1606 (m), 1554 (s), 1483 (s), 1417 (s), 1287 (m), 1225 (m), 1104 (m), 1028 (w), 896 (w), 792 (w), 736 (w), 661 (w), 596 (m), 459 (w) cm^{-1}.

$[Mn_5Nd_8(\mu_3\text{-}OH)_{12}(L^2)_4(piv)_{12}(NO_3)_4(OAc)_4]^-[H_3L^2]^+\cdot$ 7MeCN (3·7MeCN). Yield: 45 mg (53% based on Mn). Anal. Calcd for $C_{108}H_{220}Mn_5N_9Nd_8O_{66}$ (dried): C, 31.41; H, 5.36; N, 3.05. Found: C, 30.94; H, 5.03; N, 3.02. Selected IR data (KBr disk): 3611 (s), 3328 (b), 2971 (s), 2927 (m), 2868 (m), 1586 (s), 1546 (s), 1483 (s), 1413 (s), 1225 (m), 1099 (m), 1029 (w), 936 (m), 898 (w), 790 (w), 738 (w), 605 (m), 570 (m) cm^{-1}.

$[Mn_5Sm_8(\mu_3\text{-}OH)_{12}(L^2)_4(piv)_{12}(NO_3)_4(OAc)_4]^-[H_3L^2]^+\cdot$ 8MeCN (4·8MeCN). Yield: 54 mg (63% based on Mn). Anal. Calcd for $C_{108}H_{220}Mn_5N_9O_{66}Sm_8$ (dried): C, 31.04; H, 5.30; N, 3.01. Found: C, 31.09; H, 4.95; N, 3.21. Selected IR data (KBr disk): 3616 (m), 3528 (b), 2972 (s), 2928 (m), 1587 (s), 1556 (s), 1483 (s), 1402 (s), 1373 (m), 1295 (m), 1225 (m), 1100 (m), 1081 (w), 1030 (w), 936 (w), 666 (w), 610 (w), 572 (w), 463 (w) cm^{-1}.

$[Mn_5Gd_8(\mu_3\text{-}OH)_{12}(L^2)_4(piv)_{12}(NO_3)_4(OAc)_4]^-[H_3L^2]^+\cdot$ 5MeCN (5·5MeCN). Yield: 31 mg (36% based on Mn). Anal. Calcd for $C_{108}H_{220}Mn_5Gd_8N_9O_{66}$ (dried): C, 30.64; H, 5.23; N, 2.97. Found: C, 30.39; H, 5.41; N, 3.11. Selected IR data (KBr disk): 3620 (m), 3546 (b), 2975 (s), 2928 (m), 1588 (s), 1559 (s), 1483 (s), 1402 (s), 1373 (m), 1299 (m), 1225 (m), 1101 (m), 1083 (w), 1031 (w), 936 (w), 665 (w), 616 (m), 573 (m), 464 (w) cm^{-1}.

$[Mn_5Tb_8(\mu_3\text{-}OH)_{12}(L^2)_4(piv)_{12}(NO_3)_4(OAc)_4]^-[H_3L^2]^+\cdot$ 6MeCN (6·6MeCN). Yield: 49 mg (57% based on Mn). Anal. for $C_{108}H_{220}Mn_5N_9O_{66}Tb_8$ (dried) Calc. (Found): C 30.54; H, 5.22; N 2.96. Found: C, 30.24; H, 4.97; 3.22. Selected IR data (KBr disk): 3386 (b), 2961 (s), 1558 (s), 1483 (s), 1408 (s), 1374 (m), 1297 (m), 1226 (m), 1104 (m), 1030 (w), 896 (w), 741 (w), 666 (w), 611 (w), 471 (w) cm^{-1}.

X-ray Crystallography. The five isomorphous compounds **2**−**6** crystallized as pale brown plates. The structure of **5** [Mn_5Gd_8] could be determined using a conventional Mo-$K\alpha$ rotating-anode source, but crystals of the remaining four compounds were very thin (that of **3** [Mn_5Nd_8] only 4 μm thick!) and data sets were measured to 0.85 Å resolution on the SCD beamline of the ANKA synchrotron at the Forschungszentrum Karlsruhe, using Si-monochromated radiation of wavelength λ = 0.80000 Å. Data were collected at 150 K, using Stoe IPDS II area detector (**2** [Mn_5Pr_8], **3** [Mn_5Nd_8], **5** [Mn_5Gd_8], **6** [Mn_5Tb_8]) or Bruker SMART Apex CCD (**4** [Mn_5Sm_8]) diffractometers, and were corrected semiempirically[26,27] for absorption (Table 1).

(26) Sheldrick, G. M. *SHELXTL 6.14*; Bruker AXS Inc.: Madison, WI, 2003.

(27) Sheldrick, G. M. *SADABS, the Siemens Area Detector Absorption Correction*; University of Göttingen: Göttingen, Germany, 1996.

Scheme 3. Synthesis of Compounds **2**−**6**

$$H_2L^2 \xrightarrow[Ln(NO_3)_3\cdot 6H_2O/MeCN]{Mn(OAc)_2\cdot 4H_2O/HO_2CCMe_3} [Mn^{III}_5Ln^{III}_8(OH)_{12}(L^2)_4(piv)_{12}(NO_3)_4(OAc)_4]^-[H_2L^2H]^+$$

(Ln = Pr, **2**; Nd, **3**; Sm, **4**; Gd, **5**; Tb, **6**)

Structure solution by direct methods and full-matrix least-squares refinement against F^2 (all data) were carried out using SHELXTL.[26] Atomic form factors for λ = 0.80000 Å (15.510 keV) were obtained by the method of Brennan and Cowan[28] as implemented on http://skuld.bmsc.washington.edu/scatter/AS_periodic.html.

All ordered non-H atoms were refined anisotropically. The organic countercation and several of the ligand ^{t}Butyl groups showed 2-fold disorder and were refined with partial occupancy atoms. Geometrical and similarity (for thermal parameters) restraints were used as necessary within the disordered groups. O−H bond lengths were restrained. Eight MeCN molecules per cluster could be located and refined isotropically in the structure of **4** (Mn_5Sm_8). In the remaining structures the solvent molecules were disordered, and some or all could not be refined satisfactorily and were handled using the SQUEEZE option in PLATON.[29] The total number of MeCN molecules (refined and/or calculated) per complex was five for **2** (Mn_5Pr_8), seven for **3** (Mn_5Nd_8), eight for **4** (Mn_5Sm_8), five for **5** (Mn_5Gd_8), and six for **6** (Mn_5Tb_8).

Crystallographic data (excluding structure factors) for the structures in this paper have been deposited with the Cambridge Crystallographic Data Centre as supplementary publication no. CCDC 693908−693912. Copies of the data can be obtained, free of charge, on application to CCDC, 12 Union Road, Cambridge CB2 1EZ, UK: http://www.ccdc.cam.ac.uk/perl/catreq/catreq.cgi, e-mail: data_request@ccdc.cam.ac.uk, or fax: +44 1223 336033.

Magnetic Measurements. The magnetic susceptibility measurements were obtained with the use of a Quantum Design SQUID magnetometer MPMS-XL. This magnetometer works between 1.8 and 400 K for direct current (dc) applied fields ranging from −7 to 7 T. Measurements were performed on polycrystalline samples of 3.68, 9.63, 16.00, 14.65, and 1.83 mg for **2** [Mn_5Pr_8], **3** [Mn_5Nd_8], **4** [Mn_5Sm_8], **5** [Mn_5Gd_8] and **6** [Mn_5Tb_8], respectively. Alternating current (ac) susceptibility measurements have been measured with an oscillating ac field of 3 Oe and ac frequencies ranging from 1 to 1500 Hz. M vs H measurements were performed at 100 K to check for the presence of ferromagnetic impurities that have been found absent. The magnetic data were corrected for the sample holder and the diamagnetic contribution.

Results and Discussion

Synthesis. Previously, we reported the synthesis, crystal structures, and magnetic properties of high nuclearity [$Fe^{III}_5Ln^{III}_8$] (Ln = Pr, Nd, Gd) complexes obtained from the reaction of *N*-^{n}Butyldiethanolamine with the {Fe_3O} pivalate triangular complex, $Ln(NO_3)_3\cdot 6H_2O$ and $NaOAc\cdot 3H_2O$ in MeCN.[22] While the [$Fe^{III}_5Gd^{III}_8$] complex exhibited a large spin ground state (slightly lower than the maximum of 81/2) resulting from predominant ferromagnetic interactions between the spin carriers, no evidence of SMM behavior was observed above 1.8 K. The result prompted us to extend this work to the analogous Mn^{III} systems since the $3d^4$ Mn^{III} ion has a large ground state spin (S = 2) but also a significant uniaxial anisotropy arising from the Jahn−Teller distortion. We were able to synthesize and characterize compounds of composition $[Mn^{III}_5Ln^{III}_8(\mu_3\text{-}OH)_{12}(L^2)_4(piv)_{12}(NO_3)_4(OAc)_4]^-[H_2L^2H]^+\cdot n$solvent (Ln = Pr, **2**; Nd, **3**; Sm, **4**; Gd, **5**, Tb, **6**). Compounds **2**−**6** were obtained from the reaction of H_2L^2 with $Mn(OAc)_2\cdot 4H_2O$ and $Ln(NO_3)_2\cdot 6H_2O$ in the presence of pivalic acid in MeCN (Scheme 3). It should be mentioned at this point that all attempts to synthesize the Dy^{III} (that usually displays high magnetic anisotropy), Y^{III} (diamagnetic), or any other Ln^{III} analogues, under either the same or modified reaction conditions, (e.g., employing differing reactant ratios or different reaction solvents such as MeOH, EtOH, CH_2Cl_2, or a mixture thereof) were unsuccessful.[30] We found, however, that the reaction of H_2L^2 with $Ce^{III}(NO_3)_3\cdot 6H_2O$ or $(NH_4)_2[Ce^{IV}(NO_3)_6]$ under similar reaction conditions[31] gave good yields of the $[Ce^{IV}_6Ce^{III}_2Mn^{III}_2(^t\text{Budea})_2(O_2CCMe_3)_{10}(NO_3)_2(OAc)_2]$ aggregate and when the same reaction conditions used to obtain **2**−**6** were used for $La(NO_3)_3\cdot 6H_2O$, an octanuclear complex $[Mn_4La_4(OH)_4(^t\text{Bu-dea})_4(piv)_8(NO_3)_4]$ resulted. Both these compounds will be reported elsewhere. In the magnetic analysis of families of isostructural 3d-4f aggregates, it is usually helpful to have an analogue with a diamagnetic lanthanide, so that the magnetic behavior of the 3d metals alone can be determined. It turns out that in this case, where there is no direct bridging between Mn centers, such an analogue is unnecessary, as can be seen from the uncoupled magnetic behavior of the [Mn_5Sm_8] system (see below).

Despite the difference in N-substitution of the ligand and slight modification of the synthetic methodology, the nuclearity and core topology previously observed with the [$Fe^{III}_5Ln^{III}_8$] system[22] (Figure 1) is retained with the Mn^{III} analogues. The products are primarily controlled by the molar ratio of the 3d and 4f reactants, although the reactant ratio is not necessarily expressed in the product. Noteworthy is the point that, employing 0.5−1 mmol of $Ln(NO_3)_2\cdot 6H_2O$ and longer reaction times yields the same tridecanuclear complexes. However, the heterometallic product formation is optimized using 0.8 mmol $Ln(NO_3)_2\cdot 6H_2O$ and 0.1 mmol $Mn(OAc)_2\cdot 4H_2O$ with 2 h reaction time. Also direct mixing of the reactants does not lead to the desired products, and a solution of the ligand in MeCN must be added gradually to a stirred solution of pivalic acid, $Mn(OAc)_2\cdot 4H_2O$, and $Ln(NO_3)_2\cdot 6H_2O$ in MeCN.

Description of Structures of 2−6. Single crystal X-ray analyses revealed that compounds **2**−**6** consist of an ion pair comprising a $[Mn^{III}_5Ln^{III}_8(\mu_3\text{-}OH)_{12}(L^2)_4(piv)_{12}(NO_3)_4(OAc)_4]^-$ anion and a $[H_2L^2H]^+$ cation. The structure of the anion of **2** will be discussed in detail as a representative example to facilitate comparison with the previously reported [$Fe^{III}_5Ln^{III}_8$] systems. The partially labeled structure of the anion in **2** is shown in Figure 2, and the core of the molecule is given in Figure 3. Selected bond distances and bond angles (for **2**−**6**) are listed in Tables 2 and 3, respectively. The anion of **2** consists of

(28) Brennan, S.; Cowan, P. L. *Rev. Sci. Instrum.* **1992**, *63*, 850.
(29) van der Sluis, P.; Spek, A. L. *Acta Crystallogr.* **1990**, *A46*, 194.

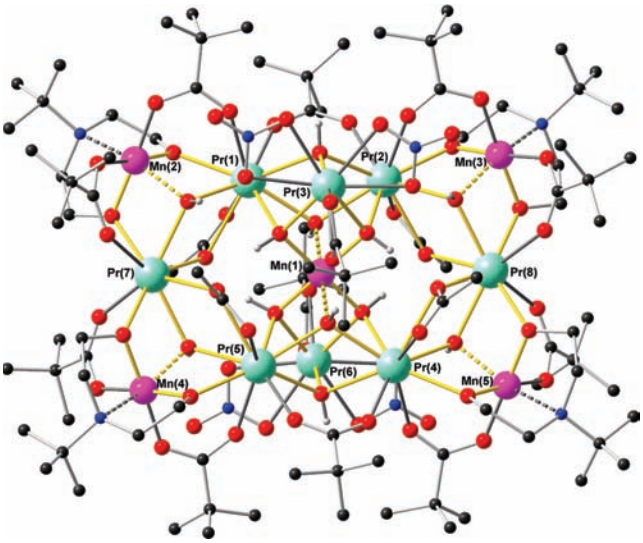

Figure 2. Molecular structure of the anion $[Mn_5^{III}Ln_8(\mu_3\text{-}OH)_{12}(L^2)_4(piv)_{12}(NO_3)_4(OAc)_4]^-$ in **2**. Hydrogen atoms, counterion and solvent molecules have been omitted for clarity. The Jahn−Teller axes of the Mn^{III} centers in **2** are shown as dotted lines. Color code: Mn (pink), Pr (light green), N (blue), O (red), C (black).

a $[Mn_5^{III}Ln_8^{III}]^{39+}$ core held together by twelve μ_3-OH^- groups. Peripheral ligation is provided by four chelating/bridging (μ_3:η^1:η^2:η^2) ^{t}Bu-dea^{2-} ligands on Mn(2), Mn(3), Mn(4), Mn(5), twelve bridging, *syn*, *syn* (μ_2:η^1:η^1) $Me_3CCO_2^-$ (piv$^-$), four chelating/bridging, *syn*, *syn*, *anti* (μ_2:η^2:η^1) $CH_3CO_2^-$ (OAc$^-$), and four chelating (μ:η^1:η^1) NO_3^- ligands on Pr(3) and Pr(6). Disregarding the differences in the side arms of the diethanolamine ligands, compounds **2**−**6** bear striking structural similarity to the previously reported $[Fe_5^{III}Ln_8^{III}]$/*N*-^{n}Butyldiethanolamine analogues,[22] as they retain the core topology represented in **1a** with the Fe^{III} centers replaced by Mn^{III} ions. The oxidation states of the Mn ions and the level of protonation of O atoms in the core of the molecule were established by charge balance considerations, bond valence sum (BVS) calculations,[32] and inspection of metric parameters such as detection of Mn^{III} Jahn−Teller elongation axes (Figures 2 and 3).

The core of this family, as exemplified by **2**, is centrosymmetric with the central Mn(1) lying on a crystallographic inversion center. The core (Figure 3) can be viewed as being composed of two distorted inner heterometallic $[Mn^{III}Pr_3^{III}(\mu_3\text{-}OH)_4]^{8+}$ cubane subunits sharing a common vertex Mn(1), flanked by four edge-sharing heterometallic $[Mn^{III}Pr_2^{III}(\mu_3\text{-}OH)_4]^{5+}$ defect cubane units. Six of the eight Pr^{III} ions (Pr(1), Pr(2), Pr(4), Pr(5), Pr(7), Pr(8)) are arranged in a planar hexagonal ring capped above and below the plane by the other two (Pr(3) and Pr(6)). The five Mn^{III} centers are close to coplanar with four Mn^{III} atoms (Mn(2), Mn(3), Mn(4), and Mn(5)) located at the vertices of a rectangle and the fifth (Mn(1)) at the center. The bridging modes within the core of the $[Mn_5^{III}Ln_8^{III}]$ analogues are identical to those of the previously reported $[Fe_5^{III}Ln_8^{III}]$ compounds.[22] Two types of bridging piv$^-$ (Pr/Pr; Pr/Mn) can be identified, the $CH_3CO_2^-$ link the ring Pr ions in the less common μ_2:η^2:η^1 fashion, and the NO_3^- ions chelate exclusively the out of plane Pr ions. Overall, each of the four peripheral Mn^{III} ions is bridged to two Pr centers by two μ_2:η^1:η^1 pivalate ligands, one μ_3-OH^- ion, and two μ_2-oxygens from a ^{t}Bu-dea^{2-} ligand, while the central Mn^{III} ion is bridged to six Pr ions through six μ_3-OH^- groups.

All the Mn^{III} ions are six-coordinate, exhibiting a distorted octahedral coordination sphere through six μ_3-OH^- ligands for the central Mn(1) atom, and an NO_5 coordination environment consisting of a NO_2 donor set from a $(L^2)^{2-}$ ligand moiety, one μ_3-OH^- group, and two bridging pivalate oxygens, for the peripheral Mn atoms. The Mn^{III} atoms exhibit Jahn−Teller distortion as expected. The distortion takes the form of an axial elongation as reflected in long *trans* bonds through the Mn^{III} ions (see Figures 2 and 3, and Table 2). The coordination bond distances in the equatorial plane are in the range of 1.893−1.945 Å, while the axial coordination bonds are elongated, 2.150 and 2.498 Å, because of the Jahn−Teller distortion.[32] The bond distances around Mn^{III} ions are typical or in the expected range of those found in octahedrally coordinated Mn^{III} complexes with N,O,O-ligation.[19a] The Mn−O bond distances range from 1.879−2.134 Å and the average Mn−N about 2.47 Å.

In contrast, the coordination spheres of the Pr centers comprise only O atoms, presenting three different types of coordination geometries, all varying in their coordination environment: (i) *Type I* (Pr(3) and Pr(6)), 9-coordinate with an O_9 coordination sphere made up of four μ-NO_3^- (η^1:η^1), three μ_3-OH^- ions and two μ-pivalates (η^1:η^1); (ii) *Type II* (Pr(1), Pr(2), Pr(4), Pr(5)), also 9-coordinate with O_9 donor set, comprising one μ_2-oxygen from a ^{t}Bu-dea^{2-} ligand, four μ_3-OH^- ions, two μ-pivalates (η^1:η^1), and two μ_2-OAc^- (η^2:η^1); (iii) *Type III* (Pr(7) and Pr(8)), with an O_8 set, bound by two μ_2-oxygens from two ^{t}Bu-dea^{2-} ligands, two μ_3-OH^- groups, two μ-piv$^-$ and two μ-OAc^- from two different pivalates and acetates, respectively. The bridged Ln−Ln separations range from 3.999 Å to 4.262 Å, while the Mn−Ln distances lie between 3.476 Å and 3.602 Å. The Ln−O−Ln bond angles within the cubanes and acetate bridges range from 104.6 to 112.0° (×16) whereas those involving O(9)−O(12) (×4) range from 116.7 to 119.1°. Meanwhile, the Mn−O−Ln bond angles involving axial J-T site on Mn (×8) range from 97.2 to 99.5° whereas those involving OH or alkoxo bridges (×20) range from 99.7 to 108.5°. The Mn centers at the corners of the complex core define an almost perfect rectangle with sides about 6.930 Å and 10.890 Å. The Mn−Mn(1)−Mn or Pr−Mn(1)−Pr (average value 179.33°) are near linear, confirming that the coordination polyhedron around the central metallic ion Mn(1) can be described in terms of a slightly distorted octahedron. Alternatively, these angles may reflect the *trans* configuration imposed by the inversion center at the central transition metal atom Mn(1). As expected, there is virtually no interaction between the molecules in the crystal as revealed by the packing diagram of **2**. A polyhedral

(30) Mereacre, V. M.; Ako, A. M.; Anson, C. E.; Powell, A. K., unpublished results.

(31) Tasiopoulos, A. J.; Milligan, P. L., Jr.; Abboud, K. A.; O'Brien, T. A.; Christou, G. *Inorg. Chem.* **2007**, *46*, 9678.

(32) Liu, W.; Thorp, H. H. *Inorg. Chem.* **1993**, *32*, 4102. The BVS are exemplarily given for the $[Mn_5Sm_8]$ analogue: Sm1 3.18, Sm2 3.24, Sm3 3.13, Sm4 3.20, Sm5 3.21, Sm6 3.24, Sm7 3.22, Sm8 3.25, Mn1 2.87, Mn2 2.92, Mn3 2.88, Mn4 2.88, Mn5 2.90, O1 1.12, O2 1.25, O3 1.28, O4 1.14, O5 1.27, O6 1.27, O7 1.17, O8 1.17, O9 1.12, O10 1.12, O11 1.11, O12 1.10.

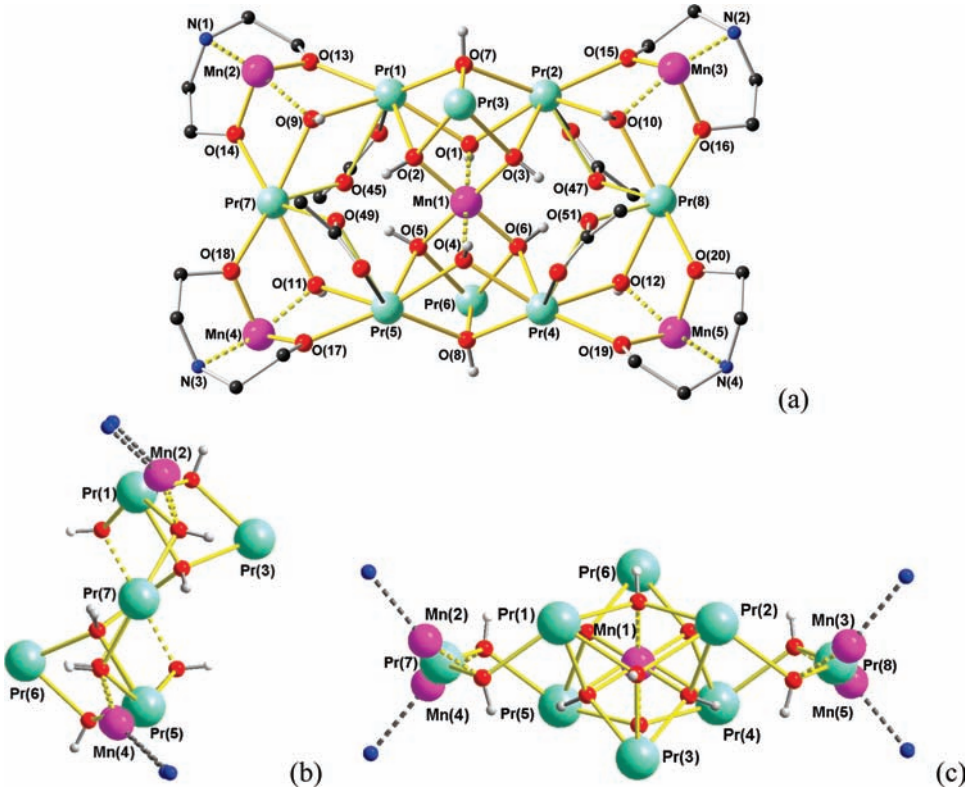

Figure 3. Core of **2**: (a) front, (b) left-hand portion and (c) from above. The Jahn−Teller axes of the Mn^{III} centers in **2** are shown as dotted lines. Color code as in Figure 2.

representation of the packing of the molecules in the crystal of **2** is given in Figure 4. The core geometry in **2**−**6** is new for Mn/4f compounds and represents a new addition to the few examples of [Mn−Ln] complexes with nuclearity exceeding 10 metal centers reported to date that are rich in both the Mn and Ln components.[10,11a,11b] While higher nuclearity heterometallic Mn-group 2 [$Mn_{13}Ca_2$], [$Mn_{14}Sr$],[33] Mn-3d [$Mn_{12}Cu_8$],[34] [$Mn_{28}Cu_{17}$],[20] Mn-5f [$Mn_{10}Th_6$],[35] and Mn-4f[10,11a,11b] complexes have been reported, tridecameric Mn-4f complexes are particularly rare.[11c,12,21,22] While the concept of substituting a 3d metal ion with another in the same structural motif is known in several examples of isostructural homometallic clusters, such as the series of nonanuclear M^{II} (M = Co,[36] Ni,[37] Fe[38]) complexes presenting the same core topology reported by Perlepes and co-workers, the application of this concept in heterometallic clusters (here replacing Fe^{III} with Mn^{III}) has not been demonstrated previously.

Magnetic Properties of 2−6. Direct current magnetic susceptibility measurements were carried out on polycrystalline powder samples of **2**−**6** in the 1.8−300 K temperature range. The plots of χT vs T data at 1000 Oe are shown in Figure 5. As can be seen in Table 4, the χT products at room temperature or the Curie constant (obtained fitting the χT vs T data to a Curie−Weiss law) are all in relatively good agreement with the expected value of isolated spins[39] and with the presence of five $S = 2$ Mn^{III} and eight Ln^{III} metal ions. When the temperature is lowered, three different types of behavior are observed, but none of them leads to a well-defined ground state as can be seen at low temperature by the absence of clear saturation on the χT product. This result highlights the presence of weak intramolecular magnetic interactions between Mn^{III} and Ln^{III} metal ions. Furthermore, the magnetic properties of **4** allow us to conclude that the intramolecular interactions between Mn^{III} spins are negligible as the χT product is independent of temperature down to 1.8 K, that is, it follows a simple Curie law. Increasing the applied magnetic field, the magnetization increases smoothly at low fields as usually observed for isolated spins, but then in a linear manner above 2 T without saturation even at 7 T (where it reaches 17.4 μ_B which is still below the magnetization value of 20 μ_B for five $S = 2$ Mn^{III} spins). This high field behavior reveals

(33) As usually observed for octahedral Mn^{III} ions, the Jahn-Teller distortion leads to elongated axial bonds (2.184(4)−2.459(4) Å). Miyasaka, H.; Clérac, R.; Wernsdorfer, W.; Lecren, L.; Bonhomme, C.; Sugiura, K.; Yamashita, M. *Angew. Chem., Int. Ed.* **2004**, *43*, 2801.

(34) Mishra, A.; Yano, J.; Pushkar, Y.; Yachandra, V. K.; Abboud, K. A.; Christou, G. *Chem. Commun* **2007**, 1538.

(35) Yamashita, S.; Shiga, T.; Kurashina, M.; Nihei, M.; Nojiri, H.; Sawa, H.; Kakiuchi, T.; Oshio, H. *Inorg. Chem.* **2007**, *46*, 3810.

(36) Mishra, A.; Abboud, K. A.; Christou, G. *Inorg. Chem.* **2006**, *45*, 2364.

(37) (a) Tsohos, A.; Dionyssopoulou, S.; Raptopoulou, C. P.; Terzis, A.; Bakalbassis, E. G.; Perlepes, S. P. *Angew. Chem., Int. Ed.* **1999**, *38*, 983. (b) Papaefstathiou, G. S.; Perlepes, S. P.; Escuer, A.; Vicente, R.; Font-Bardia, M.; Solans, X. *Angew. Chem., Int. Ed.* **2001**, *40*, 884.

(38) Papaefstathiou, G. S.; Escuer, A.; Vicente, R.; Font-Bardia, M.; Solans, X.; Perlepes, S. P. *Chem. Commun.* **2001**, 2414.

(39) (a) Boudalis, A. K.; Donnadieu, B.; Nastopoulos, V.; Clemente-Juan, J. M.; Mari, A.; Sanakis, Y.; Tuchagues, J.-P.; Perlepes, S. P. *Angew. Chem., Int. Ed.* **2004**, *43*, 2266. (b) Boudalis, A. K.; Sanakis, Y.; Clemente-Juan, J. M.; Donnadieu, B.; Nastopoulos, V.; Mari, A.; Coppel, Y.; Tuchagues, J.-P.; Perlepes, S. P. *Chem. −Eur. J.* **2008**, *14*, 2514.

(40) Benelli, C.; Gatteschi, D. *Chem. Rev.* **2002**, *102*, 2369.

Table 2. Selected Bond Distances (Å) [a] for Compounds **2**−**6**

	2 (Mn_5Pr_8)	**3** (Mn_5Nd_8)	**4** (Mn_5Sm_8)	**5** (Mn_5Gd_8)	**6** (Mn_5Tb_8)
Mn(1)−O(1)	2.176(5)	2.156(6)	2.167(3)	2.164(4)	2.165(7)
Mn(1)−O(2)	1.944(5)	1.961(6)	1.946(3)	1.941(4)	1.938(6)
Mn(1)−O(3)	1.941(5)	1.954(6)	1.946(3)	1.935(4)	1.941(7)
Mn(1)−O(4)	2.166(5)	2.153(6)	2.163(3)	2.169(4)	2.166(7)
Mn(1)−O(5)	1.940(5)	1.955(6)	1.942(3)	1.933(4)	1.943(7)
Mn(1)−O(6)	1.944(5)	1.959(6)	1.947(3)	1.950(4)	1.937(6)
Mn(2)−O(9)	2.150(5)	2.134(6)	2.129(3)	2.139(4)	2.129(7)
Mn(2)−O(13)	1.893(5)	1.883(6)	1.884(3)	1.890(4)	1.878(7)
Mn(2)−O(14)	1.921(5)	1.925(6)	1.928(3)	1.920(5)	1.920(7)
Mn(2)−N(1)	2.433(7)	2.436(8)	2.430(4)	2.421(6)	2.416(9)
Mn(3)−O(10)	2.133(5)	2.134(6)	2.126(3)	2.134(4)	2.122(7)
Mn(3)−O(15)	1.887(5)	1.879(6)	1.889(3)	1.887(5)	1.894(7)
Mn(3)−O(16)	1.922(5)	1.927(6)	1.923(3)	1.919(4)	1.921(6)
Mn(3)−N(2)	2.498(6)	2.503(7)	2.485(4)	2.486(5)	2.466(8)
Mn(4)−O(11)	2.125(5)	2.121(6)	2.122(3)	2.128(5)	2.116(7)
Mn(4)−O(17)	1.876(6)	1.885(7)	1.888(3)	1.885(5)	1.901(8)
Mn(4)−O(18)	1.935(6)	1.940(6)	1.938(3)	1.922(5)	1.933(7)
Mn(4)−N(3)	2.453(7)	2.423(8)	2.425(4)	2.417(6)	2.407(10)
Mn(5)−O(12)	2.136(5)	2.124(6)	2.123(3)	2.136(4)	2.128(7)
Mn(5)−O(19)	1.895(5)	1.885(6)	1.887(3)	1.887(5)	1.879(7)
Mn(5)−O(20)	1.926(5)	1.938(6)	1.931(3)	1.918(5)	1.917(7)
Mn(5)−N(4)	2.456(7)	2.440(7)	2.433(4)	2.430(6)	2.440(9)
Ln(1)−O(1)	2.483(5)	2.469(5)	2.347(3)	2.422(4)	2.380(6)
Ln(1)−O(2)	2.562(5)	2.533(5)	2.506(3)	2.487(4)	2.468(7)
Ln(1)−O(7)	2.531(5)	2.521(6)	2.484(3)	2.468(4)	2.455(6)
Ln(1)−O(9)	2.500(5)	2.496(5)	2.471(3)	2.451(4)	2.443(6)
Ln(1)−O(13)	2.479(5)	2.477(5)	2.440(3)	2.421(4)	2.410(6)
Ln(1)−O(45)	2.697(5)	2.686(6)	2.673(3)	2.669(5)	2.640(7)
Ln(2)−O(1)	2.448(4)	2.449(6)	2.411(3)	2.388(4)	2.395(6)
Ln(2)−O(3)	2.534(5)	2.517(5)	2.476(3)	2.461(4)	2.445(7)
Ln(2)−O(7)	2.574(5)	2.547(6)	2.532(3)	2.504(4)	2.287(7)
Ln(2)−O(10)	2.526(5)	2.519(5)	2.494(3)	2.482(4)	2.467(6)
Ln(2)−O(15)	2.468(4)	2.463(6)	2.429(3)	2.406(4)	2.388(6)
Ln(2)−O(47)	2.678(5)	2.663(5)	2.653(3)	2.633(4)	2.633(6)
Ln(3)−O(2)	2.513(5)	2.492(6)	2.460(3)	2.441(4)	2.423(7)
Ln(3)−O(3)	2.518(5)	2.495(5)	2.459(3)	2.450(4)	2.417(6)
Ln(3)−O(7)	2.378(5)	2.367(6)	2.328(3)	2.317(4)	2.287(7)
Ln(4)−O(4)	2.460(5)	2.459(5)	2.423(3)	2.411(4)	2.387(6)
Ln(4)−O(6)	2.553(5)	2.518(6)	2.494(3)	2.477(4)	2.455(6)
Ln(4)−O(8)	2.542(5)	2.530(6)	2.495(3)	2.483(4)	2.476(7)
Ln(4)−O(12)	2.546(5)	2.535(5)	2.505(3)	2.486(4)	2.488(6)
Ln(4)−O(19)	2.443(5)	2.435(6)	2.414(3)	2.403(4)	2.398(7)
Ln(4)−O(51)	2.706(5)	2.688(6)	2.683(3)	2.665(5)	2.635(7)
Ln(5)−O(4)	2.446(5)	2.443(6)	2.403(3)	2.377(4)	2.363(6)
Ln(5)−O(5)	2.558(5)	2.533(5)	2.505(3)	2.489(4)	2.467(6)
Ln(5)−O(8)	2.548(5)	2.524(6)	2.504(3)	2.478(4)	2.460(7)
Ln(5)−O(11)	2.509(5)	2.504(6)	2.482(3)	2.470(4)	2.449(7)
Ln(5)−O(17)	2.457(5)	2.444(6)	2.416(3)	2.399(4)	2.378(7)
Ln(5)−O(49)	2.687(5)	2.684(6)	2.670(3)	2.657(5)	2.655(7)
Ln(6)−O(5)	2.507(5)	2.484(6)	2.451(3)	2.434(4)	2.414(7)
Ln(6)−O(6)	2.500(5)	2.486(6)	2.449(3)	2.427(4)	2.408(7)
Ln(6)−O(8)	2.382(5)	2.367(6)	2.334(3)	2.318(4)	2.286(7)
Ln(7)−O(9)	2.447(5)	2.457(5)	2.407(3)	2.397(4)	2.373(6)
Ln(7)−O(11)	2.459(5)	2.454(6)	2.416(3)	2.412(4)	2.406(6)
Ln(7)−O(14)	2.433(5)	2.406(6)	2.370(3)	2.358(4)	2.333(7)
Ln(7)−O(18)	2.410(5)	2.398(6)	2.366(3)	2.347(5)	2.333(7)
Ln(7)−O(45)	2.506(5)	2.491(6)	2.462(3)	2.433(4)	2.450(7)
Ln(7)−O(49)	2.524(5)	2.501(6)	2.471(3)	2.444(4)	2.426(7)
Ln(8)−O(10)	2.433(5)	2.411(5)	2.388(3)	2.385(4)	2.368(6)
Ln(8)−O(12)	2.425(5)	2.431(5)	2.398(3)	2.382(4)	2.372(6)
Ln(8)−O(16)	2.443(5)	2.435(6)	2.395(3)	2.379(4)	2.363(6)
Ln(8)−O(20)	2.420(5)	2.397(6)	2.369(3)	2.355(4)	2.317(7)
Ln(8)−O(47)	2.510(5)	2.481(5)	2.457(3)	2.430(4)	2.419(6)
Ln(8)−O(51)	2.517(5)	2.515(6)	2.471(3)	2.449(4)	2.451(6)

[a] Mn−N, and Mn−O, and Ln−O involving bridging oxygens.

the presence of a significant magnetic anisotropy in this system as expected using Mn^{III} metal ions.

For **3** and **2**, the χT product first decreases before reaching a minimum at 11 K (20.7 cm^3 K/mol) and 12 K (20.2 cm^3 K/mol), respectively, and then finally increases to reach 26.9 cm^3 K/mol and 31.0 cm^3 K/mol at 1.8 K, respectively. This thermal behavior and the obtained negative Weiss constants (Figure 5, Table 4) suggest the presence of dominant but weak antiferromagnetic interactions between spin carriers within the

Table 3. Mn−O−Ln and Ln−O−Ln Bond Angles (deg) for Compounds **2**−**6**

	2 (Mn_5Pr_8)	**3** (Mn_5Nd_8)	**4** (Mn_5Sm_8)	**5** (Mn_5Gd_8)	**6** (Mn_5Tb_8)
Mn(1)−O(1)−Ln(1)	101.08(19)	101.2(2)	100.90(11)	100.61(16)	101.1(3)
Mn(1)−O(1)−Ln(2)	100.63(19)	100.7(2)	100.21(11)	100.34(16)	99.7(3)
Ln(1)−O(1)−Ln(2)	110.78(19)	110.2(2)	111.05(11)	110.90(16)	111.4(2)
Mn(1)−O(2)−Ln(1)	105.3(2)	104.8(2)	105.01(12)	105.20(18)	105.1(3)
Mn(1)−O(2)−Ln(3)	105.47(19)	105.6(2)	105.26(12)	105.33(17)	105.3(3)
Ln(1)−O(2)−Ln(3)	105.56(18)	105.85(19)	105.66(10)	105.64(15)	105.6(2)
Mn(1)−O(3)−Ln(2)	104.8(2)	104.4(2)	104.70(12)	104.87(18)	104.8(3)
Mn(1)−O(3)−Ln(3)	105.38(19)	105.7(2)	105.30(11)	105.17(17)	105.5(3)
Ln(2)−O(3)−Ln(3)	105.67(18)	105.54(19)	105.96(11)	105.67(15)	105.9(2)
Mn(1)−O(4)−Ln(4)	101.79(19)	101.2(2)	101.00(11)	100.64(16)	100.6(3)
Mn(1)−O(4)−Ln(5)	101.27(19)	101.2(2)	100.79(11)	100.73(16)	100.8(3)
Ln(4)−O(4)−Ln(5)	111.40(19)	110.7(2)	111.40(11)	111.52(17)	112.0(2)
Mn(1)−O(5)−Ln(5)	104.2(2)	104.1(2)	103.99(12)	104.10(18)	104.1(3)
Mn(1)−O(5)−Ln(6)	105.36(19)	105.8(2)	105.44(12)	105.46(17)	105.1(3)
Ln(5)−O(5)−Ln(6)	105.61(18)	105.79(19)	105.84(10)	105.72(16)	105.7(2)
Mn(1)−O(6)−Ln(4)	105.3(2)	105.0(2)	105.15(12)	105.04(18)	105.3(3)
Mn(1)−O(6)−Ln(6)	105.51(19)	105.6(2)	105.34(12)	105.16(17)	105.4(3)
Ln(4)−O(6)−Ln(6)	104.65(18)	104.8(2)	105.05(10)	105.12(15)	105.2(2)
Ln(1)−O(7)−Ln(2)	105.31(17)	105.5(2)	105.43(10)	105.65(15)	105.4(2)
Ln(1)−O(7)−Ln(3)	110.78(18)	110.2(2)	110.56(11)	110.22(16)	110.4(2)
Ln(2)−O(7)−Ln(3)	108.74(18)	108.6(2)	108.24(11)	108.45(16)	108.2(2)
Ln(4)−O(8)−Ln(5)	105.54(18)	105.8(2)	105.80(11)	105.83(16)	105.8(3)
Ln(4)−O(8)−Ln(6)	108.59(18)	108.1(2)	108.64(11)	108.39(16)	108.4(3)
Ln(5)−O(8)−Ln(6)	109.84(18)	109.7(2)	109.57(11)	109.78(16)	110.1(3)
Ln(1)−O(9)−Ln(7)	117.4(2)	116.7(2)	117.86(11)	118.27(17)	118.8(3)
Mn(2)−O(9)−Ln(1)	98.5(2)	98.5(2)	98.47(11)	98.41(16)	98.4(3)
Mn(2)−O(9)−Ln(7)	98.29(18)	98.0(2)	98.48(11)	97.88(16)	98.5(3)
Ln(2)−O(10)−Ln(8)	116.91(19)	116.9(2)	117.35(12)	117.38(17)	117.4(3)
Mn(3)−O(10)−Ln(2)	98.05(19)	98.0(2)	97.87(11)	97.52(16)	97.9(3)
Mn(3)−O(10)−Ln(8)	99.36(18)	99.7(2)	99.43(11)	98.61(16)	99.1(3)
Ln(5)−O(11)−Ln(7)	117.7(2)	117.3(2)	118.07(12)	118.27(19)	118.2(3)
Mn(4)−O(11)−Ln(5)	98.1(2)	97.9(2)	97.54(11)	97.27(17)	98.0(3)
Mn(4)−O(11)−Ln(7)	99.0(2)	98.8(2)	98.87(11)	98.08(17)	98.3(3)
Ln(4)−O(12)−Ln(8)	118.0(2)	117.9(2)	118.42(11)	119.04(17)	118.5(2)
Mn(5)−O(12)−Ln(4)	97.71(19)	97.8(2)	97.84(11)	97.72(17)	97.3(2)
Mn(5)−O(12)−Ln(8)	99.07(17)	98.6(2)	98.71(11)	98.21(17)	98.3(2)
Mn(2)−O(13)−Ln(1)	106.8(2)	106.7(2)	106.96(13)	107.04(19)	107.3(3)
Mn(2)−O(14)−Ln(7)	105.6(2)	106.0(3)	105.88(13)	105.9(2)	106.4(3)
Mn(3)−O(15)−Ln(2)	107.4(2)	107.6(2)	107.27(12)	107.67(19)	107.6(3)
Mn(3)−O(16)−Ln(8)	105.5(2)	105.2(3)	105.44(12)	105.39(18)	105.5(3)
Mn(4)−O(17)−Ln(5)	107.3(2)	107.1(3)	106.88(13)	107.1(2)	107.0(3)
Mn(4)−O(18)−Ln(7)	106.5(2)	106.2(3)	106.25(13)	106.7(2)	106.5(3)
Mn(5)−O(19)−Ln(4)	108.5(2)	108.5(2)	108.19(13)	108.24(19)	108.1(3)
Mn(5)−O(20)−Ln(8)	105.6(2)	105.4(2)	105.61(13)	105.80(19)	106.8(3)
Ln(1)−O(45)−Ln(7)	108.64(19)	109.1(2)	108.84(10)	109.23(17)	109.0(3)
Ln(2)−O(47)−Ln(8)	109.08(18)	109.6(2)	109.37(10)	110.38(16)	109.6(2)
Ln(5)−O(49)−Ln(7)	109.26(19)	109.4(2)	109.50(11)	110.39(17)	110.1(2)
Ln(4)−O(51)−Ln(8)	109.27(19)	109.6(2)	109.59(10)	110.19(17)	110.4(2)

complex core (ferrimagnetic arrangement) even if the thermal depopulation of the Ln^{III} excited states might also contribute partially to the χT decrease.[41] The magnetization measured as a function of the dc field below 10 K shows the absence of saturation even at 7 T in both compounds, which confirms the lack of well-defined ground states and also, as observed in **4**, the presence of a significant magnetic anisotropy. The magnetization, M, reaches 25.7 and 19.3 μ_B at 7 T for **3** and **2**, respectively (Figure 6).

Concerning **6** and **5**, the χT product is first roughly constant on lowering the temperature and then slightly increases below 20 K to reach 161 and 112 cm^3 K/mol at 1.8 K, respectively. This behavior and the positive Weiss constants deduced from the Curie−Weiss fit (Figure 5, Table 4), indicate the presence of dominating but weak ferromagnetic interactions within the aggregate core. The presence of ferromagnetic interactions is also supported by the rapid increase at low fields of the magnetization below 10 K (Figure 7). While M reaches 56.7 μ_B at 7 T for **6**, the saturation value for **5** at 7 T is 74 μ_B in very good agreement with the presence of eight $S = 7/2$ Gd^{III} and five $S = 2$ Mn^{III} aligned with the dc field suggesting a possible $S = 38$ ground state for this complex. As shown in **4**, the anisotropy of the Mn^{III} metal ions does not allow us to model these data with simple Brillouin functions. Nevertheless, it is worth noting that the sum of the M vs H experimental data for **4** that should roughly account for the magnetic contribution from the five Mn^{III} and eight $S = 7/2$ Brillouin functions is reproducing relatively well the experimental data (Figure 7 left). This remark emphasizes the weak amplitude of the ferromagnetic interactions in **5** as already pointed by the Weiss constant (+0.6 K) and the presence of thermally populated excited states even at 1.8 K. The presence of a significant

(41) (a) Figuerola, A.; Ribas, J.; Llunell, M.; Casanova, D.; Maestro, M.; Alvarez, S.; Diaz, C. *Inorg. Chem.* **2005**, *44*, 6939. (b) Kahn, M. L.; Sutter, J.-P.; Golhen, S.; Guionneau, P.; Ouahab, L.; Kahn, O.; Chasseau, D. *J. Am. Chem. Soc.* **2000**, *122*, 3413.

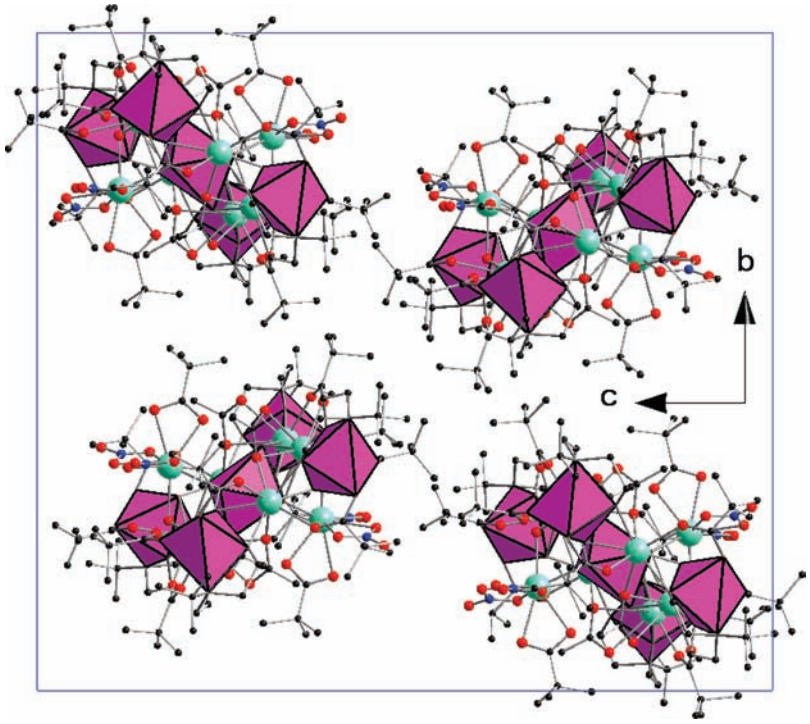

Figure 4. Polyhedral representation of the packing of **2**. Polyhedral view along the *a* axes and [−1 1 −1] direction. Organic H atoms are omitted for clarity. Color code: Mn (pink), Pr (light-green), O (red), N (blue), C (black).

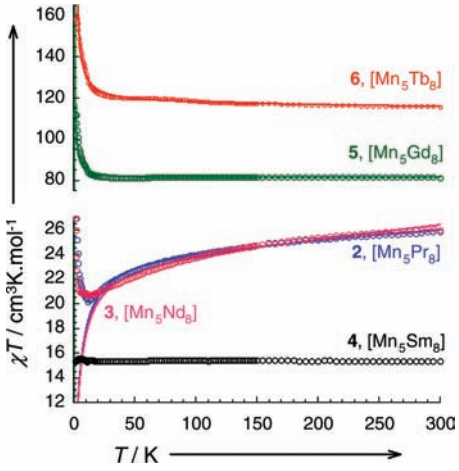

Figure 5. Temperature dependence of the χT products for **2**−**6** at 1000 Oe (with $\chi = M/H$). The solid lines are the best fit obtained using a Curie−Weiss law above 30 K for **2** and **3** and down to 1.8 K for **5** and **6**. The values of the obtained Curie and Weiss constants are given in Table 4. It is worth noting that a simple Curie behavior is seen for **4**.

magnetic anisotropy is also seen in **6** as shown by the high field linear variation of the magnetization.

A more detailed analysis of the magnetic properties is however not possible considering (i) the number of magnetic pathways for exchange between spin carriers in such molecular aggregates (see molecular structure above); (ii) the presence of Pr^{III}, Nd^{III}, Sm^{III} or Gd^{III}, Tb^{III}, lanthanide ions that cannot be easily modeled; and because (iii) the intracomplex magnetic interactions remain weak between Mn^{III} and Ln^{III} metal ions and thus excited states might be populated even at 1.8 K. Nevertheless, the ac susceptibility of these compounds in zero dc field was measured to probe the presence of magnetization slow relaxation (i.e., Single-Molecule Magnet properties). In agreement with the *M* vs *H* data at 1.8 K that do not show any sign of hysteresis effects, the ac susceptibility have shown a complete absence of out-of-phase component confirming that these complexes do not behave as SMMs above 1.8 K.

Given that our initial reason for preparing the Mn^{III} analogues of our previously published [Fe^{III}_5-Ln_8] compounds was to introduce suitable anisotropy to increase the chance of magnetic slow relaxation, we now need to consider possible reasons for what at first sight seems a disappointing lack of such behavior. We have shown above that the magnetic coupling in the [Mn_5Gd_8], and presumably also in the other analogues, seems to be either extremely weak or non-existent. For the individual Jahn−Teller based anisotropies of the Mn^{III} centers to contribute to the overall molecular anisotropy, it is first necessary that there should be some significant coupling between the metal centers within the molecule. Why, then are they in fact essentially decoupled? Considering the large numbers of Mn−O−Ln and Ln−O−Ln angles in Table 3, the lack of variation is rather striking. For the Ln−O−Ln angles, sixteen (involving the hydroxo bridges in the cubanes and the bridging acetates) fall in the rather narrow range 104.6−112.0°, with only four more in the range 116.7−119.1°. Similarly, considering the Mn−O−Ln bridges that involve equatorial sites on Mn, we again find a similarly narrow range of angles: 99.7−108.5°, and even those involving axial Jahn−Teller sites, 97.2−99.5°, do not extend the range much. Magnetic coupling between metal centers is dependent on the angle at the bridging atom, and for a given pair of metal ions there will generally be an angle at which the coupling switches from ferromagnetic, through zero, to antiferromagnetic. It is tempting to conclude that for both types of angles, Ln−O−Ln or Mn−O−Ln, the geometries observed in

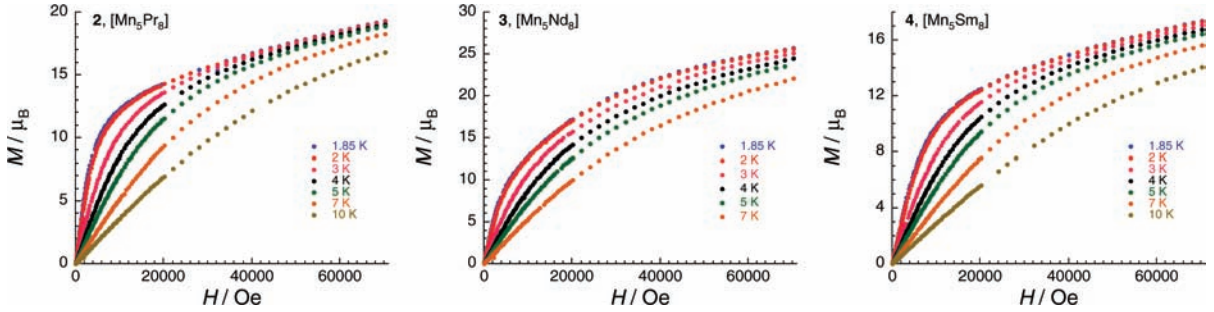

Figure 6. Field dependence of the magnetization at low temperatures for **2**−**4**.

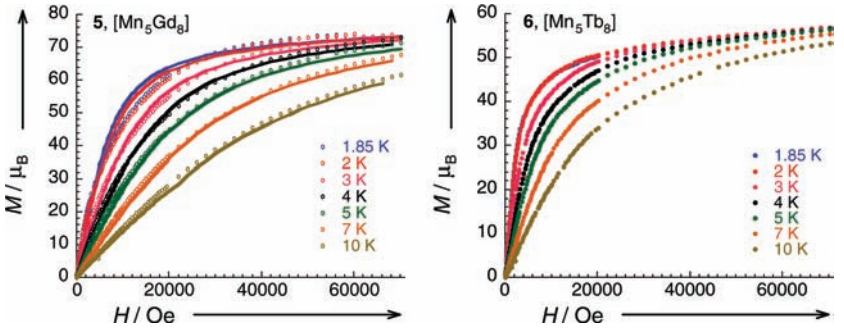

Figure 7. Field dependence of the magnetization at low temperatures for **5** (left) and **6** (right). The solid lines for **5** are the simulations of the magnetization summing the data of **4** and eight $S = 7/2$ Brillouin functions.

Table 4. Magnetic Parameters Extracted from the Data

compounds	Curie constant expected for each Ln in cm^3 K/mol [40]	Curie constant expected for $[Mn_5Ln_8]$ in cm^3 K/mol	χT measured at 300 K in cm^3 K/mol	experimental Curie constant in cm^3 K/mol	θ (K)
2, $[Mn_5Pr_8]$	1.60	27.80	25.8	23.6	−2.6
3, $[Mn_5Nd_8]$	1.64	28.12	26.1	22.7	−1.9
4, $[Mn_5Sm_8]$	0.09	15.72	15.3	15.4	0
5, $[Mn_5Gd_8]$	7.875	78.00	81	80.1	+0.6
6, $[Mn_5Tb_8]$	11.815	109.52	115.5	117.4	+1.1

the present complexes are such that the couplings are very close to zero and that the angles in the present compounds fall in a "magnetic death zone". One can compare the $[Mn_5Tb_8]$ compound, with its uniform angles, near-zero magnetic coupling, and lack of any slow relaxation, with our previously reported $[Mn_5Tb_4]$ aggregate.[19a] In the latter, the Mn−O−Tb angles show a much wider spread, 82.5−120.7°, with most of these to one side or other of our purported "death zone". In this case, the metal centers are now significantly coupled, and the energy barrier for magnetic relaxation is among the highest for 3d-4f single-molecule magnets. If we have thus (serendipitously) found the zero-point for Ln−O−Ln and Mn−O−Ln magneto-structural correlations, the challenge is now to extend it to either side. The molecular anisotropy is recognized as the critical factor determining the energy barrier for slow relaxation, but this can only be the tensor sum of the individual metal ion anisotropies if the metal ions are themselves significantly coupled.

Conclusions

We have used ^{t}Bu-deaH$_2$ to prepare the Mn^{III} analogues of our previously reported[22] $[Fe_5^{III}Ln_8]$ aggregates. The latter had been synthesized using the closely related ^{n}Bu-deaH$_2$, but it was necessary to switch to the ^{t}Butyl-substituted ligand to obtain the Mn compounds. Complexes **2**−**6** are the first high-nuclearity 3d-4f aggregates reported to date using ^{t}Bu-deaH$_2$ as ligand. Furthermore, we have demonstrated that it is possible to take a known (for Fe^{III}) 3d-4f core motif and produce the Mn^{III} analogue. This is important in helping to assess the contributions of the individual components of 3d-4f systems to the overall magnetic behavior. These compounds show no evidence of slow relaxation behavior above 1.8 K, which appears to be the consequence of the very weak or non-existent magnetic interactions between the Mn^{III} and Ln^{III} ions, resulting from the particular angles at the bridging oxygens. These systems seem to define the zero-points for any Mn−O−Ln and Ln−O−Ln magneto-structural correlations, which represent important contributions in the quest for 3d-4f SMMs.

Acknowledgment. This work was supported by the DFG (SPP 1137 and CFN), Alexander von Humboldt Foundation (V.M.), MAGMANet (Grant NMP3-CT-2005-515767), the Conseil Régional d'Aquitaine, the Université of Bordeaux, and the CNRS.